

Model for the alpha and beta shear-mechanical properties of supercooled squalane

Tina Hecksher, Niels Boye Olsen, and Jeppe C. Dyre
*"Glass and Time", IMFUFA, Dept. of Science and Environment,
Roskilde University, P. O. Box 260, DK-4000 Roskilde, Denmark*
(Dated: January 19, 2017)

This paper presents data and a model for supercooled squalane's frequency-dependent shear modulus covering frequencies from 10 mHz to 30 kHz and temperatures from 168 K to 190 K; measurements are also reported for the glass phase down to 146 K. The data reveal a strong mechanical beta process, even above the glass transition. The model focuses on the metastable equilibrium liquid phase for which the data are fitted by an electrical equivalent-circuit characterized by additivity of the dynamic shear compliances of the alpha and beta processes. The nontrivial parts of the alpha and beta processes are modeled by a "Cole-Cole retardation element" defined as a series connection of a capacitor and a constant-phase element; this results in the Cole-Cole compliance function well-known from dielectrics. The model, which assumes that the high-frequency decay of the alpha shear compliance loss varies with (angular) frequency as $\omega^{-1/2}$, has seven free parameters. Assuming time-temperature superposition for the alpha and the beta processes separately, the number of parameters varying with temperature is reduced to four. The model provides a significantly better fit to data than a similar seven-parameter Havriliak-Negami type model. From the temperature dependence of the best-fit model parameters the following conclusions are drawn: 1) the alpha relaxation time conforms to the shoving model; 2) the beta relaxation loss-peak frequency is almost temperature independent; 3) the alpha compliance magnitude (which in the model equals the inverse of the instantaneous shear modulus) is only weakly temperature dependent; 4) the beta compliance magnitude decreases upon cooling by a factor of three in the temperature range studied. The final part of the paper briefly presents measurements of the dynamic adiabatic bulk modulus covering frequencies from 10 mHz to 10 kHz in the temperature range 172 K to 200 K. These data are qualitatively similar to the shear data by having a significant beta process, and the alpha and beta bulk modulus processes both occur at frequencies similar to those of the shear modulus. A single-order-parameter framework is suggested to rationalize these similarities.

I. INTRODUCTION

Many organic liquids are easily supercooled and good glass formers, usually with the glass transition taking place far below room temperature. These systems are experimentally convenient for studying the physics of highly viscous liquids, the glass transition, glassy relaxation, etc, phenomena that are believed to be universal for basically all liquids [1–8]. As the liquid is cooled, its relaxation time and viscosity increase by many orders of magnitude over a narrow temperature range. Beyond the dominant and slowest “alpha” relaxation process many liquids have additional faster relaxation(s), notably the so-called beta relaxation. The alpha and beta relaxation processes are often studied by means of dielectric spectroscopy. They are also present, however, in the liquid’s mechanical properties, which are the focus of the present paper that presents data and model for squalane’s shear- and bulk-mechanical properties.

Squalane is a liquid alkane consisting of a linear C_{24} backbone with six symmetrically placed methyl groups. Its systematic name is 2,6,10,15,19,23-hexamethyltetracosane. Squalane is a van der Waals liquid that is an excellent glass former [1, 9–12]. Measurements of squalane’s dynamic shear modulus in the MHz range were reported many years ago [13]. Squalane’s melting point is $T_m = 235$ K and its glass transition temperature $T_g \cong 168$ K follows the well-known rule $T_g \sim (2/3)T_m$ [5, 14]. Squalane has low toxicity and is used in cosmetics as moisturizer; due to the complete saturation squalane is not subject to auto-oxidation [15]. In basic research squalane is used as reference liquid in tribology and for elucidating the mechanism of elasto-hydrodynamic friction [16–19]. Squalane has been studied in molecular dynamics simulations of nonlinear flows [20]. Squalane has also been used as a solvent for studying the intriguing Debye dielectric relaxation of mono-hydroxy alcohols [21], the rotation of aromatic hydrocarbons in viscous alkanes [22], and the Stokes-Einstein relation for diffusion of organic solutes [23]. Due to its low vapor pressure squalane is used as a benchmark molecule for reaction-dynamics experiments performed under ultrahigh vacuum [24, 25].

Studies of neat supercooled squalane include measurements of its dielectric relaxation [10] and dynamic shear modulus in the quasistatic region over frequencies from a few mHz to 10 Hz [9], later extended to frequencies up to 30 kHz [11]. The present paper covers the latter range of frequencies with more accurate data for more temperatures than Ref. 11. The main motivation is not to present new data, however, but to introduce an electrical equivalent-circuit model representing data very well; the new model is an extension of a model discussed previously by our group [26].

Section II presents the data and the piezo-ceramic transducer used to obtain them. Section III introduces electrical-equivalent circuit modeling of linear mechanical relaxation phenomena in general and arrives at the model used for interpreting data. The model has four free parameters and three “shape” parameters that are fixed from data at one temperature. Section IV shows that the model fits data very well, in fact considerably better than a Havriliak-Negami type model with the same number of free parameters. While the main focus is on the dynamic shear data, Sec. V supplements these by presenting some dynamic bulk-modulus data. Finally, Sec. VI gives a discussion with a focus on the temperature dependence of the best-fit model parameters, showing that these conform to the showing model and that the beta process activation energy is temperature independent. If these two findings were built into the model, it would just have two parameters varying with temperature.

II. DATA FOR THE DYNAMIC SHEAR MODULUS

This paper focuses on the modeling of the dynamic shear-mechanical properties of metastable equilibrium supercooled liquid squalane above 168 K. Measurements were performed, however, at temperatures down to 146 K, which is well into the glass. Data were obtained with 2 K intervals using the three-disk piezo-ceramic shear transducer shown in Fig. 1(a) [27] in the setup described in Ref. 28. The cryostat keeps temperature stable within 10 mK. References 29 and 30 give details about the home-built cryostat and impedance-measuring setup.

Initially the filled transducer was annealed at the highest temperature for 30 hours in order to equilibrate the ceramics. After this each temperature was monitored by spending one hour for equilibration before performing a measurement, which lasts approximately one hour. The measurement was repeated to ensure reproducibility, i.e., that the liquid is in metastable equilibrium and that the setup works properly. The protocol is illustrated in Fig. 1(b). After all measurements had finished, the empty transducer was calibrated [28]. If everything works, a set of data as those analyzed below may be obtained within less than a week.

Figure 2(a) and Fig. 2(b) present the data for the real and imaginary parts of the dynamic shear modulus $G(\omega)$ in which ω is the angular frequency. The figure shows in Fig. 2(c) a so-called Nyquist plot of $G(\omega)$, i.e., real versus imaginary parts parametrized by the frequency; in this figure data for the glassy phase were included. Figure 2(d) and Fig. 2(e) present the real and imaginary parts of the dynamic shear compliance $J(\omega) = 1/G(\omega)$, while Fig. 2(f) gives the Nyquist plot of $J(\omega)$.

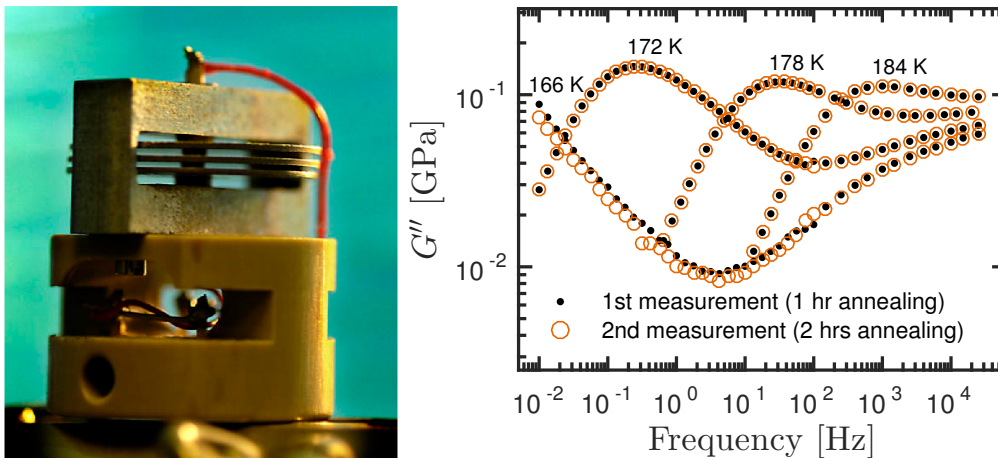


FIG. 1. (a) Three-disc transducer used for measuring the dynamic shear modulus over frequencies from 1 mHz to 50 kHz (above which resonances make it impossible to measure in the quasi-static mode) [27]. This paper presents data from 10 mHz to 30 kHz. The discs are polarized piezo-ceramics with electrodes on both sides that are electrically coupled in such a way that when the middle disc expands radially, the upper and lower discs contract by half the amount [27]. Each disc has thickness 0.5 mm and diameter 20 mm. The liquid is placed between discs 1 and 2 and between discs 2 and 3 at a high temperature at which squalane has low viscosity. (b) Data for the imaginary part of the shear modulus as a function of frequency, $G''(\omega)$, illustrating the measurement protocol: Starting at a high temperature a series of data were generated by moving in steps of 2 K down to 146 K. At each temperature the sample was equilibrated for one hour before measuring, which takes approximately another hour when the lowest frequency is 10 mHz. The procedure was repeated to ensure reproducibility and that the sample is in thermal equilibrium. The 166 K data show that equilibrium was not reached. We do not analyze data below 168 K, but above this temperature the liquid is in a state of metastable equilibrium and there is full reproducibility.

III. ELECTRICAL-EQUIVALENT CIRCUIT MODEL

A. Philosophy of circuit modeling

Many scientists regard the modeling of linear-response data by an electrical equivalent circuit as old-fashioned. A common argument is that all data may be fitted by an electrical circuit and that, consequently, such type of models can contribute little if physical insight is the goal. In our opinion this skepticism is not fair [32], and the following reasons may be given for using electrical equivalent circuits for rationalizing data:

- *Physical consistency.* Circuit models guarantee that inconsistencies are avoided. Not only is *linearity* ensured, so is *causality* and *positive dissipation*, requirements that any linear-response model must obey.
- *Simplicity.* The electrical circuit defines the model. Even simple circuits usually summarize several differential equations.
- *Same language as that used for modeling the experimental setup.* This paper is concerned with the interpretation of linear-response data for the dynamic shear modulus. The experimental setup used for obtaining these data is itself modeled by an electrical equivalent circuit [28–30], and there is an element of economy in using electrical equivalent circuits for both purposes.
- *High- and low-frequency limits.* These limits are straightforward to identify for a given circuit.
- *Couplings between different linear-response functions are easily introduced.* A major challenge for research into glass-forming liquids is to understand the relation between different frequency-dependent linear-response functions like the shear and bulk moduli, dielectric constant, specific heat, etc [33]. Such relations are conveniently modeled via electrical equivalent circuits related by transformers in which, for instance, charge is transformed into mechanical displacement or entropy, electrical current into velocity (shear rate) or heat current over temperature, and voltage into mechanical force or temperature [34, 35]. Transitions between the different physical situations are represented by transformer elements with the property that the power – the product of “voltage” and “current” – is invariant. For more on the general so-called energy bond graph formalism the reader is referred to Refs. 34–38; a very brief discussion is given below.

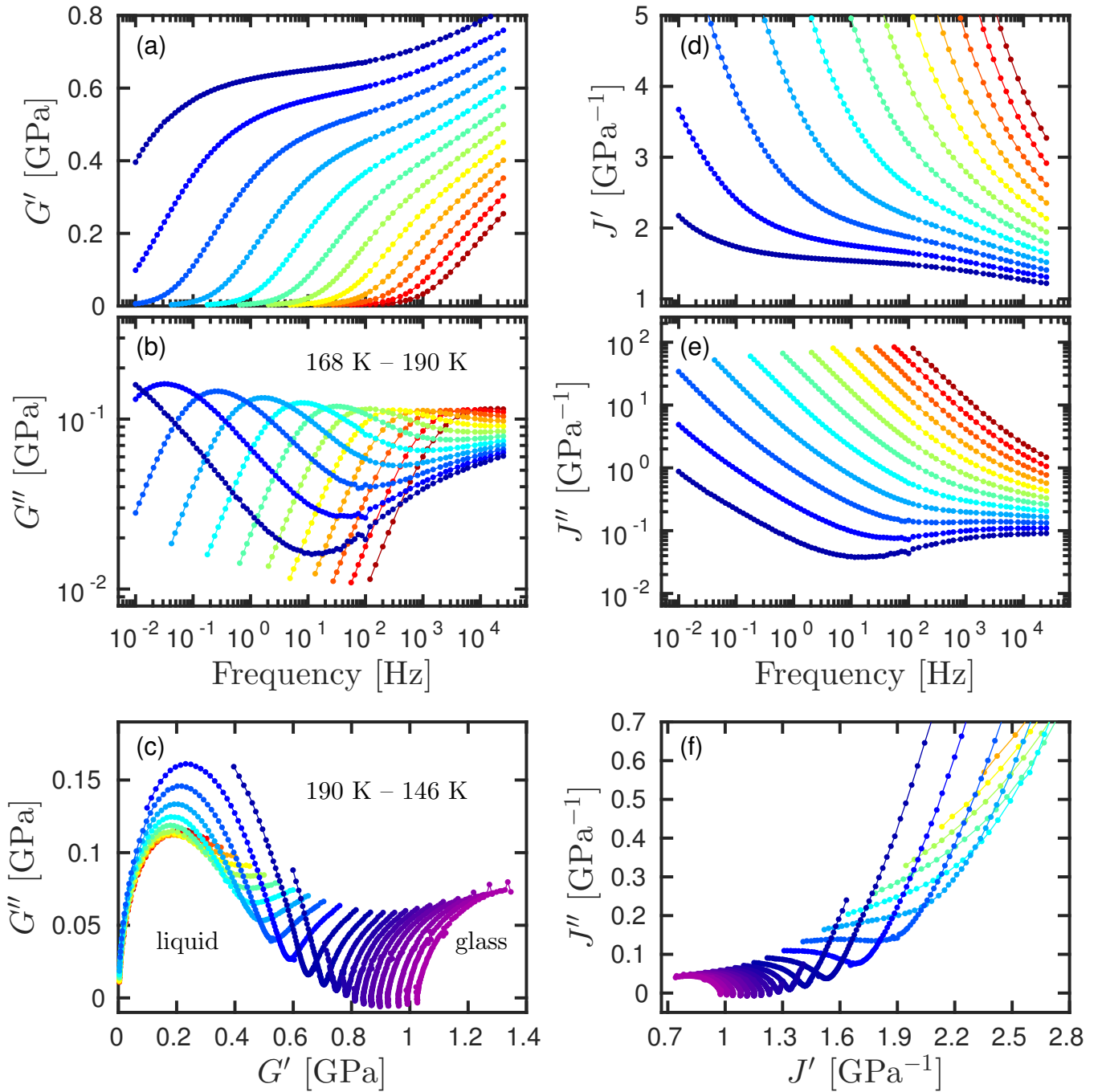


FIG. 2. The dynamic shear modulus $G(\omega)$ and shear compliance $J(\omega) = 1/G(\omega)$ of the metastable equilibrium supercooled liquid phase of squalane for temperatures ranging from 168 K to 190 K probed at intervals of 2 K [31]. The blue symbols correspond to low temperatures, the red ones to high temperatures. (a) and (b) show the real and imaginary parts of $G(\omega) \equiv G'(\omega) + iG''(\omega)$. (c) shows the so-called Nyquist plot of $G(\omega)$, i.e., the real part along the x axis and the imaginary part along the y axis in a curve parametrized by the frequency; we here included data extending into the glassy state where only the β process is observable. (d) and (e) show the real and negative imaginary parts of $J(\omega) \equiv J'(\omega) - iJ''(\omega)$; (f) shows the Nyquist plot of $J(\omega)$ (excluding the highest temperatures).

- *Straightforward extension to a nonlinear model via parametric control.* The electrical equivalent circuit's parameters vary with the thermodynamic state point. Having such dependencies controlled by charges or voltages at particular points of the circuit opens for constructing simple models of physical aging, which automatically ensure that no fundamental physical laws are violated.

Once an electrical equivalent circuit has been constructed that represents data accurately, this provides an important input for constructing a microscopic physical model of the system in question. We regard the circuit as a help towards eventually obtaining the ultimate microscopic understanding, not as the final model itself.

B. Basic circuit elements

Rheology has its own circuit language based on dashpots representing Newtonian viscous flow and springs representing a purely elastic response [39]. This language is mathematically equivalent to electrical circuit modeling. Which language to use is a matter of convenience, but as physicists we are more used to the language of electrical circuits. This has the advantage of easily relating to dielectric relaxation phenomena, which are of great importance for glass-forming liquids [40] and closely connected to the shear-mechanical properties [41–44].

Translating from electrical to rheological circuits is a bit counterintuitive when it comes to the diagrammatic representation because series connections become parallel connections and *vice versa*: since two elements in series in an electrical circuit have the *same current*, this corresponds to the analogous rheological elements being placed *in parallel* because the two shear displacements are identical. Likewise, an electrical-circuit *parallel* connection translates into a mechanical *series* connection. Once this is kept in mind, however, translation between the two languages is straightforward and unique.

This paper uses electrical equivalent circuits to model of dynamic mechanical relaxation phenomena. For this reason below we do not distinguish between the dynamic capacitance $C(\omega)$ and the dynamic shear compliance $J(\omega)$. There is as mentioned a general circuit modeling language – the so-called energy-bond graph formalism [34–37] – which may be used also, e.g., for thermal relaxation phenomena. An energy bond is characterized by an “effort” variable e and a “flow” variable f , the product of which gives the power transferred into the system from its surroundings. For a thermodynamic energy bond e is the temperature deviation from a reference temperature and f is the entropy current (heat flow over temperature) [34, 45, 46].

How to translate electrical linear-response functions to the corresponding rheological ones? With the general energy-bond language in mind, the generalized displacement q represents electrical charge or shear displacement (strain), the generalized flow given by $f \equiv \dot{q}$ represents electrical current or shear rate, and the generalized effort e represents voltage drop or shear stress [34, 36, 37]. The most important complex-valued linear-response functions translate as follows when given as functions of the angular frequency ω in the standard way (e.g., $q(t) = \text{Re}[q(\omega) \exp(i\omega t)]$ in which $q(\omega)$ is a complex amplitude):

- Electrical capacitance $C(\omega)$ corresponds to the complex shear compliance $J(\omega)$ since both in the Fourier domain are equal to displacement/force, i.e., $q(\omega)/e(\omega)$. If the symbol \sim is used for “corresponds to”, this is summarized follows:

$$C(\omega) \sim J(\omega) \sim \frac{q(\omega)}{e(\omega)}. \quad (1)$$

- Inverse electrical capacitance $1/C(\omega)$ corresponds to the complex shear modulus $G(\omega) = 1/J(\omega)$ since both in the Fourier domain are equal to force/displacement, i.e., $e(\omega)/q(\omega)$:

$$\frac{1}{C(\omega)} \sim G(\omega) \sim \frac{e(\omega)}{q(\omega)}. \quad (2)$$

- Electrical impedance $Z(\omega) = 1/Y(\omega)$ corresponds to the complex shear viscosity $\eta(\omega)$ since both in the Fourier domain are equal to force/velocity, i.e., $e(\omega)/\dot{q}(\omega) = e(\omega)/f(\omega) = e(\omega)/(i\omega q(\omega))$:

$$Z(\omega) \sim \eta(\omega) \sim \frac{e(\omega)}{i\omega q(\omega)}. \quad (3)$$

Three basic elements are used below: resistors, capacitors, and constant-phase elements (CPE) [47]. A CPE is characterized by a capacitance that as a function of ω varies as

$$C(\omega) \propto (i\omega)^{-x} \quad (4)$$

in which $0 < x < 1$. The name CPE reflects the fact that the ratio between the real and imaginary parts of $C(\omega)$ is the same at all frequencies, which implies a constant phase difference between displacement and force. The CPE is a generalization of capacitors and resistors because a capacitor obeys $C(\omega) \propto (i\omega)^0 = \text{Const.}$ while a resistor's capacitance is given by $C(\omega) \propto (i\omega)^{-1}$. Thus allowing for $0 \leq x \leq 1$ there is just a single ‘‘Lego block’’ in the model tool box, namely the CPE.

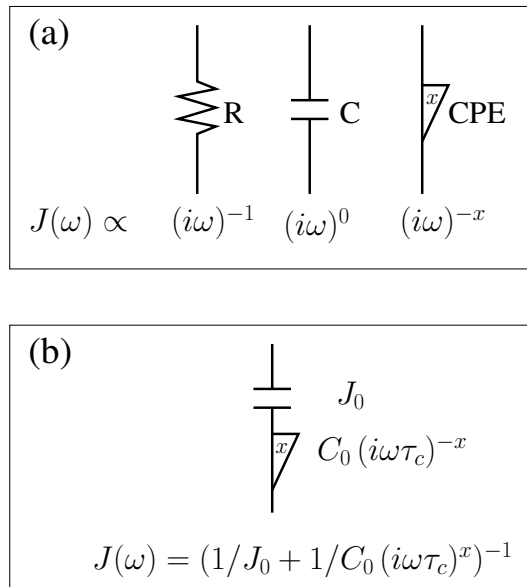


FIG. 3. Elements used here for electrical equivalent-circuit modeling. (a) The three basic elements: a resistor (R), a capacitor (C), and a constant-phase element (CPE). Their complex, frequency-dependent capacitances – corresponding to the dynamic shear compliance $J(\omega)$ (Eq. (1)) – vary with angular frequency ω in proportion to, respectively, $(i\omega)^{-1}$, $(i\omega)^0 = \text{Const.}$, and $(i\omega)^{-x}$ ($0 < x < 1$). (b) The Cole-Cole retardation element (CCRE) leading to the well-known Cole-Cole expression for the capacitance (shear compliance) Eq. (8) from 1941 [48].

Figure 3(a) shows the three basic elements. Note that Eq. (4) translates into

- $J(\omega) \propto (i\omega)^{-x}$ for the CPE dynamic shear compliance,
- $G(\omega) \propto (i\omega)^x$ for the CPE dynamic shear modulus,
- $\eta(\omega) \propto (i\omega)^{x-1}$ for the CPE dynamic shear viscosity.

C. Parametrizing the constant-phase element

For the CPE we define a magnitude constant C_0 and a characteristic time τ_c via the parametrization

$$C(\omega) = C_0 (i\omega\tau_c)^{-x}. \quad (5)$$

Because the CPE is time-scale invariant, the two constants C_0 and τ_c are not uniquely determined because the same physics is described by using instead for any number k the magnitude constant kC_0 and the characteristic time $k^{1/x}\tau$. The CPE is central for the model proposed below, and for the discussion of the model parameters' temperature dependence in fit to data (Sec. VI) we need a convention about the magnitude constant and the characteristic time. We take C_0 to be a *universal, temperature-independent* number. The motivation is that, if any physics is to be ascribed to τ_c , the CPE magnitude constant C_0 should also make sense physically. Since squalane like most other organic glass-forming liquids have an instantaneous shear modulus, i.e., high-frequency plateau modulus, of order GPa, we fix the magnitude constant as follows:

$$C_0 \equiv 1 \text{ GPa}^{-1}. \quad (6)$$

In this way, once the exponent x has been determined in a fit to data, the capacitance of a CPE element at a single frequency uniquely determines τ_c .

Physically, we think of the characteristic time τ_c as controlling the rate of the CPE element's "inner" clock in much the same sense as the material time of the Narayanaswamy physical-aging theory [49–52].

D. The Cole-Cole retardation element

What is here termed a Cole-Cole retardation element (CCRE) consists of a series connection of two of the basic circuit elements, a CPE and a capacitor (Fig. 3(b)). Recall that the capacitance $C(\omega)$ of two elements in series with capacitances $C_1(\omega)$ and $C_2(\omega)$ is given by $1/C(\omega) = 1/C_1(\omega) + 1/C_2(\omega)$. Thus if the CCRE capacitor's value is J_0 , the CCRE compliance $J(\omega)$ is given by

$$\frac{1}{J(\omega)} = \frac{1}{J_0} + \frac{1}{C_0(i\omega\tau_c)^{-x}}. \quad (7)$$

The CCRE is named after the Cole-Cole dielectric capacitance function from 1941 [48], which in the mechanical language is the following expression

$$J(\omega) = \frac{J_0}{1 + (i\omega\tau)^x}. \quad (8)$$

Here J_0 is the DC shear compliance and τ is the inverse angular loss-peak frequency. It is straightforward to show that Eq. (7) implies Eq. (8) if one defines

$$\tau = \tau_c \left(\frac{J_0}{C_0} \right)^{1/x}. \quad (9)$$

The fit to data of Sec. IV below gives CPE characteristic times τ_c that are thermally activated for both the alpha and the beta process, with an activation energy proportional to the instantaneous shear modulus for the alpha CPE characteristic time, but virtually temperature independent for the beta CPE characteristic time. Note that the characteristic time is not identical to the inverse loss-peak frequency of each process.

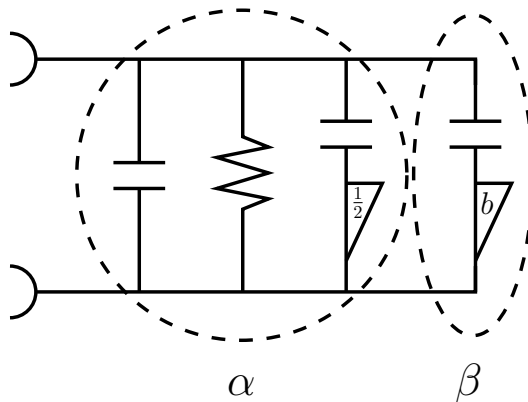


FIG. 4. The electrical equivalent-circuit model for the dynamic shear-mechanical data of squalane. The alpha process is represented by a standard RC element – corresponding to the Maxwell model Eq. (10) – in parallel with a Cole-Cole retardation element (CCRE) with exponent 1/2. The beta process is represented by an additional CCRE, and the model is characterized by additivity of the alpha and beta compliances. The model has seven parameters, one for each basic element except for the beta CPE element that has two free parameters. In the fit to data three dimensionless combinations of the seven parameters were assumed to be temperature independent, reflecting the assumption that the alpha and beta shear compliances separately obey time-temperature superposition.

E. Model for the dynamic shear-mechanical properties

To arrive at a realistic electrical equivalent circuit model of squalane's shear dynamic response, we first note that a standard electrical RC element – a resistor and a capacitor in parallel – corresponds to the classical Maxwell model for viscoelasticity. This model is based on the assumption that the stress decays exponentially to zero whenever the sample is at rest [1, 5, 53]. If the shear stress is denoted by σ , the shear (strain) displacement by γ , the DC shear viscosity by η_0 , and the instantaneous shear modulus by G_∞ , the differential equation describing the Maxwell model for any shear rate as a function of time, $\dot{\gamma}(t)$, is [1, 5, 53]

$$\dot{\gamma}(t) = \frac{\sigma(t)}{\eta_0} + \frac{\dot{\sigma}(t)}{G_\infty}. \quad (10)$$

That the Maxwell model is equivalent to an electrical RC element follows by noting that for an RC element the voltage is the same across both elements, which in the Maxwell model corresponds to the same shear stress. The resistor current corresponds to the first term on the right hand side of Eq. (10) (a dashpot in the traditional language of viscoelasticity), and the capacitor current corresponds to the second term (a spring in the viscoelastic language).

The Maxwell model is too simple to fit data for glass-forming liquids, however, and the model must be extended by including one or more non-trivial dissipative terms. It is this paper's basic assumption that these terms are described by CCREs placed in parallel to the Maxwell RC element, one for the alpha process and one for the beta process (Fig. 4).

In the model (Fig. 4) none of the two CCREs are inherently linked to the alpha process RC element. Nevertheless, one CCRE will be regarded as part of the alpha process for the following reasons. Previous publications of the *Glass and Time* group have presented experimental [28, 54, 55], as well as theoretical [56–58], evidence that in the absence of beta relaxation the alpha process has a generic $\omega^{-1/2}$ high-frequency decay of the dielectric loss and shear compliance. This is an old idea; for instance, a generic $\omega^{-1/2}$ high-frequency decay is the characteristic feature of the 1967 Barlow-Erginsav-Lamb (BEL) model [1, 53, 56, 59, 60]. Consequently, we fix the exponent to 1/2 for one CCRE and regard this element as part of the alpha process. Confirming this assignment, for liquids without a mechanical beta relaxation like the silicone diffusion pump oils DC704 and DC705, the dynamic shear compliance is well fitted by the model without the beta CCRE (unpublished).

The dynamic shear compliance is a sum of the individual elements' shear compliances. Thus the model leads to the following expression, which henceforth defines the model parametrization:

$$J(\omega) = J_\alpha \left(1 + \frac{1}{i\omega\tau_\alpha} + \frac{k_1}{1 + k_2(i\omega\tau_\alpha)^{1/2}} \right) + \frac{J_\beta}{1 + (i\omega\tau_\beta)^b}. \quad (11)$$

For later use we note that the instantaneous shear modulus $G_\infty = \lim_{\omega \rightarrow \infty} G(\omega) = \lim_{\omega \rightarrow \infty} 1/J(\omega)$ is given by

$$G_\infty = \frac{1}{J_\alpha}. \quad (12)$$

The plateau modulus between the alpha and beta processes (at temperatures low enough that these are well separated, i.e., $\omega\tau_\alpha \gg 1$ and $\omega\tau_\beta \ll 1$) is denoted by $G_{p,\alpha\beta}$ and given by

$$G_{p,\alpha\beta} = \frac{1}{J_\alpha + J_\beta}. \quad (13)$$

In the low-frequency limit the shear compliance diverges as $\propto 1/i\omega\tau_\alpha$ as required for any liquid with a finite DC viscosity. In the same limit the real part of the shear compliance, the so-called recoverable shear, is given by

$$\text{Re}(J(0)) = (1 + k_1)J_\alpha + J_\beta. \quad (14)$$

The model has seven parameters:

- two compliance strengths J_α and J_β [unit: 1/GPa],
- two relaxation times τ_α and τ_β [unit: s],

- two α “shape parameters” k_1, k_2 [dimensionless],
- the β CCRE exponent b [dimensionless].

In order to limit the number of free parameters we make the assumption that time-temperature superposition (TTS) applies separately for both the alpha and the beta processes, implying that in the fit to data the three dimensionless shape parameters k_1, k_2 , and b do not vary with temperature. The parameters allowed to vary are the two compliance strengths and the two relaxation times.

The characteristic times of the alpha and beta CPEs are denoted by $\tau_{c,\alpha}$ and $\tau_{c,\beta}$. In the below fit to data we take, as mentioned, the constants k_1 and k_2 to be independent of temperature, implying that $\tau_{c,\alpha} \propto \tau_\alpha$. For this reason the parameter $\tau_{c,\alpha}$ will not be discussed separately from τ_α . The beta characteristic time $\tau_{c,\beta}$, on the other hand, is qualitatively different from τ_β in its temperature variation, which makes this an important parameter to keep track of (Sec. VI).

IV. FITTING THE MODEL TO DATA

The model was fitted to the squalane data of Fig. 2 using MATLAB’s “fminsearch” Nelder-Mead downhill simplex least-squares fitting procedure. The fit excluded data taken at too low a temperature to be in equilibrium or at such high temperatures that the alpha and beta process have more or less completely merged. These limitations leave the data for temperatures between 168 K and 182 K for parameter identification.

The data for the real and imaginary parts of the frequency-dependent shear modulus cover angular frequencies ranging from 10 mHz to 30 kHz, with up to 16 frequencies per decade evenly distributed on a logarithmic scale. The data were fitted to Eq. (11) by proceeding as follows. First, the three temperature-independent shape parameters k_1, k_2, b were identified by fitting to the 172 K data, which have the alpha and the beta loss peaks well within the frequency window, but still clearly separated. The fit was performed for the shear-modulus, because using the shear compliance the fit would have been dominated by its low-frequency divergence.

Figure 5 compares model fits (green curves) to data (black crosses). Figure 5(a) gives model prediction versus data for the real part of the dynamic shear modulus, Fig. 5(b) gives the same for the imaginary part, and Fig. 5(c) gives model prediction versus data in a Nyquist plot of the shear modulus. Figure 5(d), Fig. 5(e), and Fig. 5(f) give the same for the dynamic shear compliance.

The fits are excellent. Given the number of free parameters this may not be surprising. Our experience with fitting data to similar models over the last 20 years show, however, that the present model is better than other models with the same number of parameters. As an illustration of the superiority of the new model, we have compared to a fit assuming a Havriliak-Negami (HN) type function for the alpha process. The function fitted to data is the following:

$$J(\omega) = J_\alpha \left(1 - \frac{1}{(1 + (i\omega\tau_\alpha^{\text{HN}})^c)^a} \right)^{-1} + \frac{J_\beta}{1 + (i\omega\tau_\beta^{\text{HN}})^b}. \quad (15)$$

The function Eq. (15) has the same number of parameters as Eq. (11): two strength parameters, two relaxation times, and three dimensionless shape parameters. There is only one qualitative difference to Eq. (11): the latter has a finite so-called recoverable compliance, i.e., low-frequency limit of $J'(\omega)$. We determined the best-fit parameters in the same way as above. The fit to data is not as good as that of Eq. (11). This is clear from Fig. 6 that compares the overall quality of the two fits as functions of temperature.

Turning back to the model Eq. (11), Fig. 7 shows the temperature variation of the four free parameters. Figure 7(a) shows how the alpha and beta relaxation times τ_α and τ_β vary with temperature. As always for a glass-forming liquid, the alpha relaxation time increases strongly when temperature decreases. The beta relaxation time is almost constant and, in fact, not even a monotonic function of temperature. In contrast, the beta *characteristic* time $\tau_{c,\beta}$ decreases systematically with temperature. The dielectric beta loss-peak frequency is usually reported to be Arrhenius [40, 63], but it is important to note that almost all literature data for τ_β (the inverse beta loss-peak frequency) refer to the glass phase, not to the metastable liquid phase about T_g . Figure 7(b) shows the best-fit shear-compliance strengths J_α and J_β . Note that the beta process strength varies considerably more than the alpha strength.

These findings are qualitatively consistent with previous ones of ours for the beta dielectric relaxation process, which may be summarized as follows [61, 62]: In the metastable liquid phase the (beta) relaxation strength increases considerably with increasing temperature whereas the relaxation time is almost temperature independent, in the glassy phase the strength is almost constant whereas the loss-peak frequency (inverse relaxation time) is strongly temperature dependent (Arrhenius). It is possible to rationalize these properties of the beta process – as well as its behavior under annealing of the out-of-equilibrium liquid – by assuming that the characteristic time $\tau_{c,\beta}$ is Arrhenius

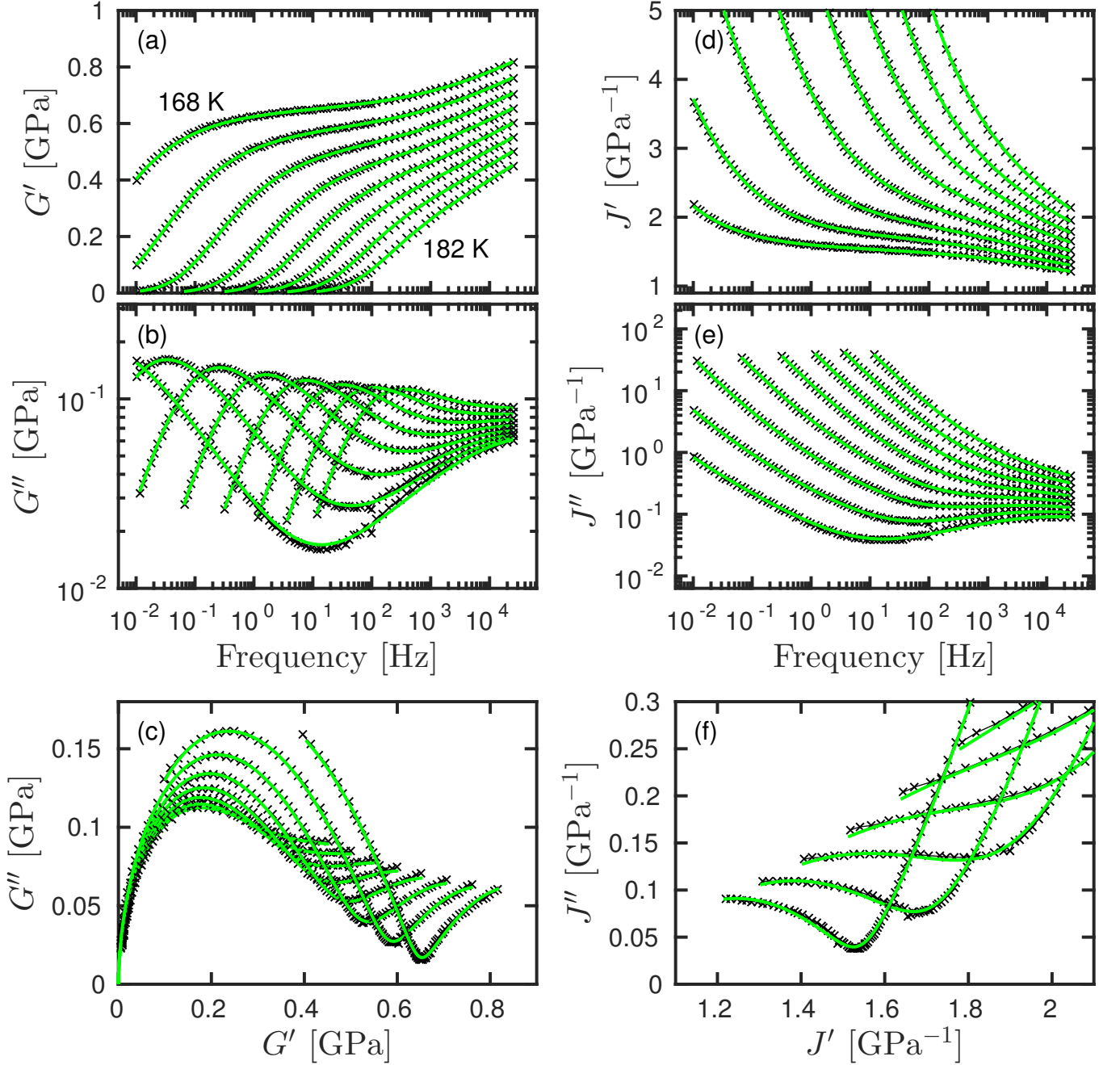


FIG. 5. Comparison between data (black crosses) and model predictions (Eq. (11), green curves). The four free parameters were determined as described in the text; the remaining three temperature-independent shape parameters k_1 , k_2 , and b were identified by fitting to the 172 K data.

both above and below the glass transition with the same activation energy, whereas the beta relaxation strength freezes at the glass transition (unpublished).

V. DATA FOR THE DYNAMIC ADIABATIC BULK MODULUS

Figure 8 shows the transducer used for measuring the dynamic adiabatic bulk modulus. It consists of a radially polarized piezo-ceramic spherical shell coated with electrodes on the inner and outer surfaces. An electrical potential induces a slight compression or expansion of the sphere volume in which the liquid is placed (the top is a reservoir

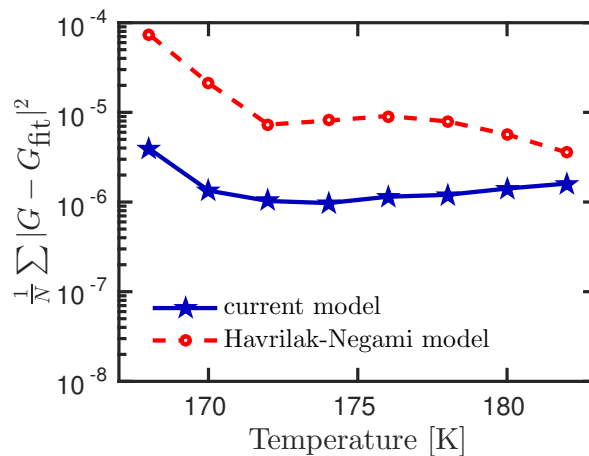


FIG. 6. Comparing the quality of fitting data to Eq. (11) and to Eq. (15) quantified via the frequency-integrated deviation of the complex shear modulus from that of the data. Although the two models have the same number of parameters, the former fits data better by at least a factor of two and more than a factor of ten at low temperatures.

allowing for the liquid’s thermal expansion) [28, 64, 65]. Figure 9 shows our data for real and imaginary parts of the dynamic adiabatic bulk modulus $K(\omega) = K'(\omega) + iK''(\omega)$, (a) and (b), as well as in a Nyquist plot, (c).

Comparing the bulk modulus loss, Fig. 9(b), to the shear modulus loss, Fig. 2(b), we see a qualitatively similar behavior with an alpha loss peak that moves rapidly to lower frequencies upon cooling and a large beta peak, which at the same time becomes visible. To the best of our knowledge this is the first observation of a clear beta process for the dynamic bulk modulus.

How to interpret the similarity between the dynamic shear and bulk moduli? This finding is fully consistent with previous ones [28, 33], but is important to remember that there is no fundamental reason for the similarity. This is because the dynamic bulk modulus – whether adiabatic or isothermal – is a *scalar* linear-response function whereas the dynamic shear modulus is a *vector* linear-response function. This means that these functions belong to fundamentally different symmetry classes, as discussed by Meixner long time ago [45]. Nevertheless, by reference to the Eshelby picture of structural rearrangements within a surrounding elastic matrix, Buchenau has recently discussed how the relaxational parts of the bulk and shear moduli may be connected [66]. His arguments may be extended to finite frequencies, thus establishing a connection between $G(\omega)$ and $K(\omega)$.

Referring to the energy-bond language [34–38], there are two fundamental thermodynamic scalar energy bonds: a thermal bond with effort equal to temperature difference and flow equal to entropy current, and a mechanical bond with effort equal to minus pressure difference and flow equal to rate of volume change. Consistent with Buchenau’s reasoning [66] we would like to propose a general energy-bond model in which all dissipation connected with the two scalar thermodynamic energy bonds is controlled by the dynamic shear modulus (or, equivalently, the dynamic shear compliance). A schematic representation of this idea is given in Fig. 10(b). An energy-bond diagram of this sort implies that the system in question is a “single-order-parameter” liquid [38, 67–69]. This is equivalent to being a so-called R simple system, i.e., one with so-called isomorphs, which are lines in the thermodynamic phase diagram along which the dynamics is invariant to a very good approximation [70–73].

In Fig. 10(b) there may be several non-dissipative elements, but the important point is that these are all connected to the element Fig. 4 via a single, internal energy bond. The predictions for the dynamic adiabatic/isothermal bulk moduli (or those of the dynamic expansion coefficient [74]) depend, of course, not just on the dynamic shear modulus (compliance), but also on the non-dissipative elements. Nevertheless, for a system described by Fig. 10 one *a priori* expects that all the scalar response functions at any given temperature have alpha and beta processes located at frequencies similar to those of the shear modulus (compliance) alpha and beta processes.

VI. DISCUSSION

This paper has demonstrated that shear-mechanical data for squalane may be fitted very well with the electrical-equivalent circuit model of Fig. 4 leading to Eq. (11) for the dynamic shear-mechanical compliance. The model assumes additivity of the alpha and beta shear compliances. The model has seven parameters, one more than alternative phenomenological models [26, 75]. In our fit to data, however, the three shape parameters were taken to be temperature independent, reflecting the assumption that time-temperature superposition applies separately to

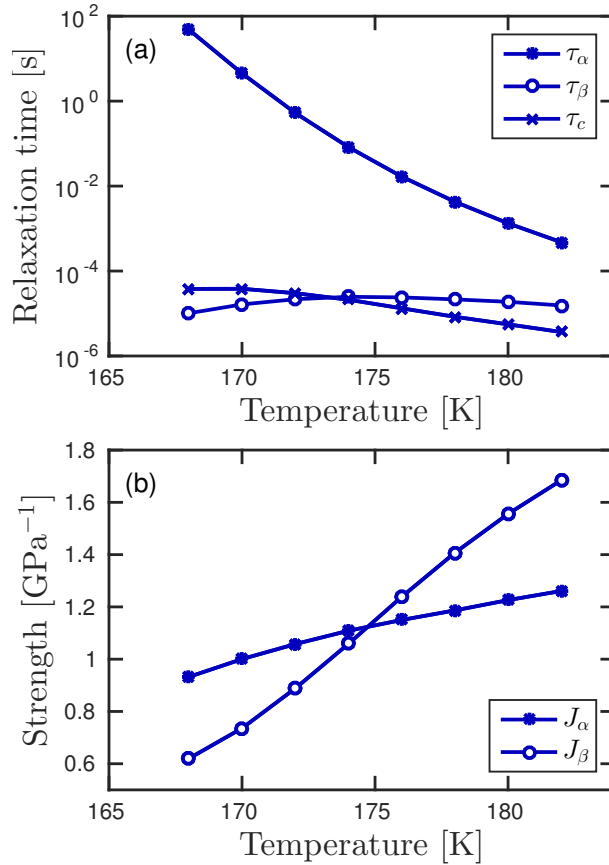


FIG. 7. Temperature dependence of the parameters when Eq. (11) is fitted to the shear-modulus data of Fig. 2 assuming temperature independence of the three shape parameters k_1 , k_2 , and b ; these were identified by fitting to the 172 K data resulting in $k_1 = 7.9$, $k_2 = 4.8$, $b = 0.36$. (a) shows the alpha and beta relaxation times, τ_α and τ_β , as well as the beta characteristic time $\tau_{c,\beta}$. Note that $\tau_{c,\beta}$ differs from τ_β and has a systematic variation with temperature. τ_α decreases strongly with increasing temperature, which is a well-known feature of glass-forming liquids. (b) shows the temperature dependence of the shear-compliance strengths J_α and J_β . The latter changes by a almost factor of three whereas J_α changes by just 25% over the same temperatures. The results of (a) and (b) for the beta process are qualitatively similar to previous findings of ours for the dielectric beta loss-peak frequency of glass-forming organic liquids, which is found to be Arrhenius in the glass phase but only weakly temperature dependent in the metastable liquid phase, whereas the beta strength has the opposite behavior with strong temperature dependence in the liquid and weak in the glass [61, 62].

both the alpha and the beta compliance functions. In this picture, the observed significant deviations from TTS derive from merging of the alpha and beta processes. We conjecture that this applies generally for glass-forming liquids.

How to physically justify that the Maxwell RC element and the two CCRES should be combined in a way that is additive in their shear compliances, not in their shear moduli? There are no logically compelling arguments for this. We think of it as follows. Imagine a small particle in the liquid. The particle's mean-square displacement (MSD) as a function of time in one axis direction, $\langle \Delta x^2(t) \rangle$, will have a rapid increase on the phonon time scale, followed by a transition to the long-time diffusive behavior proportional to time. If one assumes that the alpha and beta processes contribute independently to the particle's motion, i.e., that $\Delta x(t) = \Delta x_\alpha(t) + \Delta x_\beta(t)$ with $\langle \Delta x_\alpha(t) \Delta x_\beta(t) \rangle = 0$, the MSD will be a sum of an alpha and a beta contribution: $\langle \Delta x^2(t) \rangle = \langle \Delta x_\alpha^2(t) \rangle + \langle \Delta x_\beta^2(t) \rangle$. If one moreover assumes the Stokes-Einstein relation between dynamic shear viscosity and the particle's dynamic friction coefficient, this translates via the fluctuation-dissipation theorem into additivity of the dynamic shear compliances for the alpha and beta processes.

In regard to the single-particle MSD, note that with any function $\langle \Delta x^2(t) \rangle$ there is an associated characteristic time, the time at which the particle has moved a typical intermolecular distance. In the same way this is how we think of each CPE basic element's characteristic τ_c , which was defined as the time at which the absolute value of the compliance at $\omega = 1/\tau_c$ has the physically meaningful value 1 GPa $^{-1}$ (Eq. (6)). For the beta process, it is important to distinguish between this time and the inverse loss-peak frequency, τ_β because via Eq. (9) the latter time's temperature variation reflects the combined effect of the changing compliance strength J_β and the Arrhenius $\tau_{c,\beta}$. Incidentally,



FIG. 8. The piezo-ceramic transducer used for measuring the dynamic adiabatic bulk modulus [28–30, 64, 65]. The device consists of a piezo-electric ceramic shell coated with electrodes on both sides with wires connecting the two electrodes to a frequency analyzer. The inner diameter is 18 mm, the shell thickness is 0.5 mm. A small hole in the shell makes it possible to fill the bulk transducer with liquid at a high temperature at which the viscosity is low. A tube acting as a liquid reservoir is attached on top of the hole, which ensures that the sphere is always filled as the liquid contracts upon cooling.

these considerations give rise to a new model for the beta process, which provides an alternative to the 2003 “minimal model” [62]. We intend to return to this in a future publication.

The electrical-equivalent circuit model Fig. 4 is identical to that proposed in Ref. 26 except for an extra capacitor, the one in the alpha CCRE. This capacitor eliminates an unphysical feature of our previous model [26, 32], which predicted an infinite so-called recoverable shear compliance (the amount of return flow following a step shear displacement of size unity). This unphysical feature is also present in the BEL model from 1967 [1, 59]. Introducing the extra capacitor results in symmetry between the alpha and beta CCREs, the only difference being that the alpha CCRE has the fixed exponent 1/2 and a characteristic time that is proportional to RC in its temperature variation.

We note that if the alpha CCRE’s relaxation time is much shorter than RC , the circuit mimics the situation reported in recent papers for the dielectric relaxation of monohydroxy alcohols, for which one observes a low-frequency Debye-type process followed by, in order of increasing frequency, first an alpha and then, in most liquids, a beta process [76, 77].

As regards the temperature dependence of the model parameters we have compared to the prediction of the shoving model [5, 78]. If $\tau_0 \cong 10^{-14}$ s is a typical phonon time and V_c the so-called characteristic volume assumed to be temperature independent, the shoving model predicts the following relation between the alpha relaxation time and the instantaneous (high-frequency plateau) shear modulus G_∞ :

$$\tau_\alpha(T) = \tau_0 e^{V_c G_\infty(T)/k_B T}. \quad (16)$$

The shoving model, which links a supercooled liquid’s fragility to the temperature variation of G_∞ , fits data well for many glass-forming liquids [5, 28, 78, 79]. The shoving model relates to Eq. (11) since if the model applies, the number of temperature-dependent parameters is reduced from four to three. We have not made this assumption in the fit to data, but have instead checked Eq. (16) against the best-fit parameters. This is done in Fig. 11 in which the relaxation times τ_α and $\tau_{c,\beta}$ are converted into temperature-dependent activation energies $E(T)$ by writing $\tau(T) = \tau_0 \exp(E(T)/RT)$ with $\tau_0 = 10^{-14}$ s. According to the shoving model $E_\alpha(T) = V_c G_\infty(T)$. By comparing the black crosses and the red triangles in Fig. 11 we conclude that this model applies. If the shoving model is instead interpreted with G_∞ taken to be the plateau modulus between the alpha and beta relaxations, $G_{p,\alpha\beta}$ given by Eq. (13), however, the model does not apply (blue crosses).

Our model consists of a Maxwell element in parallel with two CCREs. One may speculate that additional high-frequency mechanical processes beyond the alpha and beta relaxations can be modelled by adding further CCREs, each CCRE still being subject to time-temperature superposition.

To summarize, an excellent fit to dynamic shear-mechanical data of squalane is provided by an electrical equivalent circuit model with seven parameters. The model assumes an $\omega^{-1/2}$ high-frequency decay of the alpha compliance [56–59], additivity of the alpha and beta compliance functions, and that these functions separately obey time-temperature superposition. The latter assumption reduces the number of parameters varying with temperature to four. The best

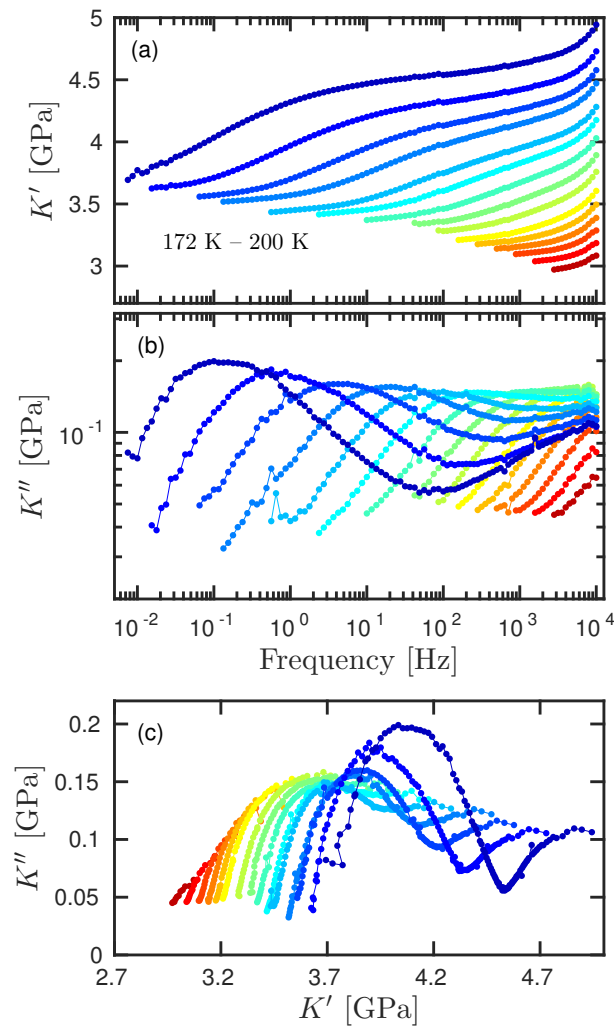


FIG. 9. Data for the dynamic adiabatic bulk modulus of squalane covering temperatures from 172 K to 200 K. (a) and (b) show the real and the imaginary parts of $K(\omega)$, respectively. (c) shows the Nyquist plot of the same data.

fit parameters confirm the showing model and show that the beta process characteristic time has a temperature-independent activation energy. If these findings were incorporated as model assumptions, the number of parameters that vary with temperature reduces to two. These could be taken to be, e.g., the compliance magnitudes J_α and J_β . We presented also data for the adiabatic dynamic bulk modulus and argued briefly that these may be interpreted qualitatively in terms of a “single-order-parameter” model in which all dissipation is controlled by the shear-mechanical properties. Such a model connects the class of scalar viscoelastic linear-response functions with that of vector symmetry [45].

In regard to future works, one obvious thing is to compare the model to shear-mechanical data for other glass-forming liquids. We have not done so systematically, but have found in all cases tested so far that the model works well (unpublished). The hope is that the model is general, thus providing a step towards a microscopic understanding of glass-forming liquids’ mechanical properties.

ACKNOWLEDGMENTS

Figure 10(b) is a special case of the general energy-bond diagram for a system with a single order parameter identified by our *Glass and Time* colleague Tage Christensen about 15 years ago, initiating a development that led

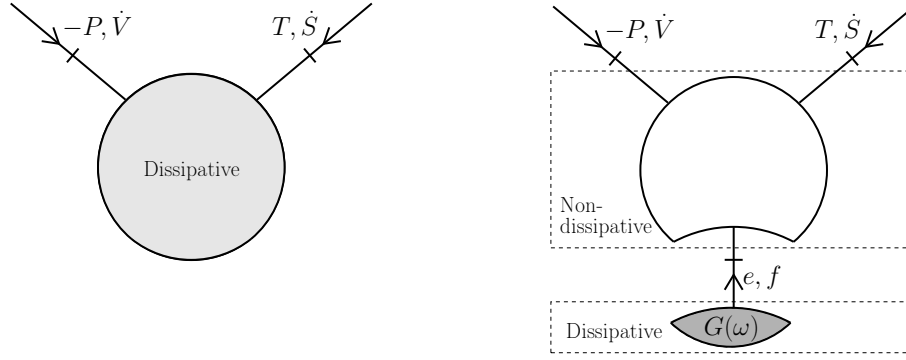


FIG. 10. Schematic energy-bond diagram for the linear dynamic responses of the two fundamental scalar thermodynamic bonds: the thermal bond defined by temperature and entropy flow and the mechanical bond defined by pressure and negative rate of volume change. The left figure shows the general scenario. The right figure shows the situation in which all dissipation is controlled by the dynamic shear modulus, a special case of the single-order-parameter scenario discussed some time ago [67]. This diagram provides a general link between the vector energy bond associated with mechanical shear deformation and the two scalar thermodynamic energy bonds. Actual predictions are only possible, of course, when a specific diagram has been constructed following this overall architecture.

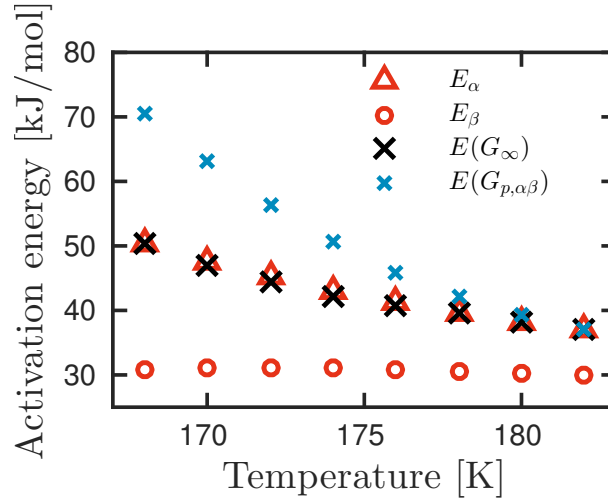


FIG. 11. Activation energies calculated from $E = RT \ln(\tau/\tau_0)$ for the alpha relaxation time τ_α (red triangles) and the beta characteristic time $\tau_{c,\beta}$ (red circles), assuming in both cases that $\tau_0 = 10^{-14}$. E_β is temperature independent to a good approximation, showing that $\tau_{c,\beta}$ is Arrhenius. The alpha relaxation time activation energy is compared to the prediction of the shoving model (black crosses) according to which $E_\alpha = V_c G_\infty$ in which V_c is the “characteristic” temperature-independent volume and G_∞ is the instantaneous, i.e., high-frequency limiting shear modulus, which according to Eq. (11) equals $1/J_\alpha$. The shoving model is confirmed. If one in this model, however, instead of G_∞ uses the plateau modulus corresponding to frequencies between the alpha and beta process, $G_{p,\alpha\beta}$ (Eq. (13)), the E_α prediction results in the blue crosses that do not fit the red triangle data. The shoving-model based activation energies $E(G_\infty)$ and $E(G_{p,\alpha\beta})$ were both normalized to predict the correct alpha activation energy at $T = 182$ K (leading to V_c being 9% of the molar volume for the $E(G_\infty)$ case).

to Ref. 67 and eventually to the isomorph theory [68, 72].

-
- [1] G. Harrison, *The Dynamic Properties of Supercooled Liquids* (Academic (New York), 1976).
 - [2] S. Brawer, *Relaxation in Viscous Liquids and Glasses* (American Ceramic Society, Columbus, OH, 1985).
 - [3] M. D. Ediger, C. A. Angell, and S. R. Nagel, “Supercooled liquids and glasses,” *J. Phys. Chem* **100**, 13200 (1996).
 - [4] C. A. Angell, “Formation of glasses from liquids and biopolymers,” *Science* **267**, 1924–1935 (1995).
 - [5] J. C. Dyre, “The Glass Transition and Elastic Models of Glass-Forming Liquids,” *Rev. Mod. Phys.* **78**, 953–972 (2006).
 - [6] L. Berthier and G. Biroli, “Theoretical Perspective on the Glass Transition and Amorphous Materials,” *Rev. Mod. Phys.*

- 83**, 587–645 (2011).
- [7] G. Floudas, M. Paluch, A. Grzybowski, and K.L. Ngai, *Molecular Dynamics of Glass-Forming Systems: Effects of Pressure* (Springer, Berlin, 2011).
- [8] F. H. Stillinger and P. G. Debenedetti, “Glass transition – thermodynamics and kinetics,” *Annu. Rev. Condens. Matter Phys.* **4**, 263–285 (2013).
- [9] R. D. Deegan, R. L. Leheny, N. Menon, S. R. Nagel, and D. C. Venerus, “Dynamic shear modulus of tricresyl phosphate and squalane,” *J. Phys. Chem. B* **103**, 4066–4070 (1999).
- [10] R. Richert, K. Duvvuri, and LT Duong, “Dynamics of glass-forming liquids. VII. Dielectric relaxation of supercooled tris-naphthylbenzene, squalane, and decahydroisoquinoline,” *J. Chem. Phys.* **118**, 1828–1836 (2003).
- [11] B. Jakobsen, K. Niss, and N. B. Olsen, “Dielectric and shear mechanical alpha and beta relaxations in seven glass-forming liquids,” *J. Chem. Phys.* **123**, 234511 (2005).
- [12] M. J. P. Comunas, X. Paredes, F. M. Gacino, J. Fernandez, J.-P. Bazile, C. Boned, J. L. Daridon, G. Galliero, J. Pauly, and K. R. Harris, “Viscosity Measurements for Squalane at High Pressures to 350 MPa from T = (293.15 to 363.15) K,” *J. Chem. Thermodyn.* **69**, 201–208 (2014).
- [13] A. J. Barlow and A. Erginsav, “Viscoelastic retardation of supercooled liquids,” *Proc. Roy. Soc.* **A327**, 175–190 (1972).
- [14] C. A. Angell, K. L. Ngai, G. B. McKenna, P. F. McMillan, and S. W. Martin, “Relaxation in glassforming liquids and amorphous solids,” *J. Appl. Phys.* **88**, 3113–3157 (2000).
- [15] Wikipedia article (2016).
- [16] Scott Bair, “Reference liquids for quantitative elastohydrodynamics: selection and rheological characterization,” *Tribol. Lett.* **22**, 197–206 (2006).
- [17] M. J. P. Comunas, X. Paredes, F. M. Gacio, J. Fernndez, J. P. Bazile, C. Boned, J. L. Daridon, G. Galliero, J. Pauly, K. R. Harris, M. J. Assael, and S. K. Mylona, “Reference correlation of the viscosity of squalane from 273 to 373 K at 0.1 MPa,” *J. Phys. Chem. Ref. Data* **42**, 033101 (2013).
- [18] Hugh Spikes and Zhang Jie, “History, origins and prediction of elastohydrodynamic friction,” *Tribol. Lett.* **56**, 1–25 (2014).
- [19] Kurt A. G. Schmidt, Doug Pagnutti, Meghan D. Curran, Anil Singh, J. P. Martin Trusler, Geoffrey C. Maitland, and Mark McBride-Wright, “New experimental data and reference models for the viscosity and density of squalane,” *J. Chem. Eng. Data* **60**, 137–150 (2015).
- [20] Scott Bair, Clare McCabe, and Peter T. Cummings, “Comparison of nonequilibrium molecular dynamics with experimental measurements in the nonlinear shear-thinning regime,” *Phys. Rev. Lett.* **88**, 058302 (2002).
- [21] L. M. Wang, S. Shahriari, and R. Richert, “Diluent effects on the Debye-type dielectric relaxation in viscous monohydroxy alcohols,” *J. Phys. Chem. B* **109**, 23255–23262 (2005).
- [22] B. Brocklehurst and R.N. Young, “Rotation of aromatic hydrocarbons in viscous alkanes. 2. Hindered rotation in squalane,” *J. Phys. Chem. A* **103**, 3818–3824 (1999).
- [23] Bruce A. Kowert and Michael B. Watson, “Diffusion of organic solutes in squalane,” *J. Phys. Chem. B* **115**, 9687–9694 (2011).
- [24] M. E. Saecker, S. T. Govoni, D. V. Kowalski, M. E. King, and G. M. Nathanson, “Molecular beam scattering from liquid surfaces,” *Science* **252**, 1421–1524 (1991).
- [25] S. P. K. Köhler, S. K. Reed, R. E. Westacott, and K. G. McKendrick, “Molecular dynamics study to identify the reactive sites of a liquid squalane surface,” *J. Phys. Chem. B* **110**, 11717–11724 (2006).
- [26] B. Jakobsen, K. Niss, C. Maggi, N. B. Olsen, T. Christensen, and J. C. Dyre, “Beta relaxation in the shear mechanics of viscous liquids: Phenomenology and network modeling of the alpha-beta merging region,” *J. Non-Cryst. Solids* **357**, 267–273 (2011).
- [27] T. Christensen and N. B. Olsen, “A rheometer for the measurement of a high shear modulus covering more than seven decades of frequency below 50 kHz,” *Rev. Sci. Instrum.* **66**, 5019–5031 (1995).
- [28] T. Hecksher, N. B. Olsen, K. A. Nelson, J. C. Dyre, and T. Christensen, “Mechanical spectra of glass-forming liquids. i. low-frequency bulk and shear moduli of DC704 and 5-PPE measured by piezoceramic transducers,” *J. Chem. Phys.* **138**, 12A543 (2013).
- [29] Brian Igarashi, Tage Christensen, Ebbe H. Larsen, Niels Boye Olsen, Ib H. Pedersen, Torben Rasmussen, and Jeppe C. Dyre, “A cryostat and temperature control system optimized for measuring relaxations of glass-forming liquids,” *Rev. Sci. Instrum.* **79**, 045105 (2008).
- [30] Brian Igarashi, Tage Christensen, Ebbe H. Larsen, Niels Boye Olsen, Ib H. Pedersen, Torben Rasmussen, and Jeppe C. Dyre, “An impedance-measurement setup optimized for measuring relaxations of glass-forming liquids,” *Rev. Sci. Instrum.* **79**, 045106 (2008).
- [31] Details about the data can be obtained from the *Glass and Time* Data repository, found online at <http://glass.ruc.dk/data>.
- [32] N. Saglanmak, A. I. Nielsen, N. B. Olsen, J. C. Dyre, and K. Nissa, “An electrical circuit model of the alpha-beta merging seen in dielectric relaxation of ultraviscous liquids,” *J. Chem. Phys.* **132**, 024503 (2010).
- [33] B. Jakobsen, T. Hecksher, T. Christensen, N. B. Olsen, J. C. Dyre, and K. Niss, “Identical temperature dependence of the time scales of several linear-response functions of two glass-forming liquids,” *J. Chem. Phys.* **136**, 081102 (2012).
- [34] P. V. Christiansen, *Dynamik og Diagrammer* (IMFUFA tekst No. 8, Roskilde University, Roskilde, 1978).
- [35] D. C. Karnopp, D. L. Margolis, and R. C. Rosenberg, *System Dynamics – Modeling and Simulation of Mechatronic Systems*, 4th ed. (Wiley, New York, 2006).
- [36] H. Paynter, *Analysis and Design of Engineering Systems* (MIT Press, Cambridge, Massachusetts, 1961).
- [37] G. Oster, A. Perelson, and A. Katchalsky, “Network thermodynamics,” *Nature* **234**, 393–399 (1971).
- [38] T. B. Schröder, N. P. Bailey, U. R. Pedersen, N. Gnan, and J. C. Dyre, “Pressure-Energy Correlations in Liquids. III.

- Statistical Mechanics and Thermodynamics of Liquids with Hidden Scale Invariance,” J. Chem. Phys. **131**, 234503 (2009).
- [39] J. D. Ferry, *Viscoelastic Properties of Polymers, 2nd Edition* (Wiley, New York, 1970).
- [40] R. Richert, “Supercooled liquids and glasses by dielectric relaxation spectroscopy,” Adv. Chem. Phys. **156**, 101–195 (2015).
- [41] E. A. DiMarzio and M. Bishop, “Connection between the macroscopic electric and mechanical susceptibilities,” J. Chem. Phys. **60**, 3802–3811 (1974).
- [42] K. Niss, B. Jakobsen, and N. B. Olsen, “Dielectric and shear mechanical relaxations in glass-forming liquids: A test of the Gemant-DiMarzio-Bishop model,” J. Chem. Phys. **123**, 234510 (2005).
- [43] U. Buchenau, “Shear and dielectric spectra in highly viscous liquids,” Phys. Rev. B **83**, 052201 (2011).
- [44] A. Garcia-Bernabe, J. V. Lidon-Roger, M. J. Sanchis, R. Diaz-Calleja, and L. F. del Castillo, “Interconversion algorithm between mechanical and dielectric relaxation measurements for acetate of *cis* - and *trans* -2-phenyl-5-hydroxymethyl-1,3-dioxane,” Phys. Rev. E **92**, 042307 (2015).
- [45] J. Meixner and H.G. Reik, “Thermodynamik der irreversiblen prozesse,” in *Prinzipien der Thermodynamik und Statistik / Principles of Thermodynamics and Statistics*, Handbuch der Physik / Encyclopedia of Physics, Vol. 2 / 3 / 2, edited by S. Flügge (Springer Berlin Heidelberg, 1959) pp. 413–523.
- [46] J. D. Bernal, “The Bakerian lecture, 1962. The structure of liquids,” Proc. R. Soc. London Ser. A **280**, 299–322 (1964).
- [47] A. K. Jonscher, *Universal Relaxation Law* (Chelsea Dielectric Press, London, 1996).
- [48] Kenneth S. Cole and Robert H. Cole, “Dispersion and absorption in dielectrics I. Alternating current characteristics,” J. Chem. Phys. **9**, 341–351 (1941).
- [49] O. S. Narayanaswamy, “A Model of Structural Relaxation in Glass,” J. Am. Ceram. Soc. **54**, 491–498 (1971).
- [50] G. W. Scherer, *Relaxation in Glass and Composites* (Wiley, New York, 1986).
- [51] Tina Hecksher, Niels Boye Olsen, and Jeppe C. Dyre, “Communication: Direct tests of single-parameter aging,” J. Chem. Phys. **142**, 241103 (2015).
- [52] J. C. Dyre, “Narayanaswamy’s 1971 aging theory and material time,” J. Chem. Phys. **143**, 114507 (2015).
- [53] J. Lamb, “Viscoelasticity and lubrication: A review of liquid properties,” J. Rheol. **22**, 317–347 (1978).
- [54] N. B. Olsen, T. Christensen, and J. C. Dyre, “Time-Temperature Superposition in Viscous Liquids,” Phys. Rev. Lett. **86**, 1271–1274 (2001).
- [55] Albena I. Nielsen, Tage Christensen, Bo Jakobsen, Kristine Niss, Niels Boye Olsen, Ranko Richert, and Jeppe C. Dyre, “Prevalence of approximate t relaxation for the dielectric process in viscous organic liquids,” J. Chem. Phys. **130**, 154508 (2009).
- [56] Jeppe C. Dyre, “Solidity of viscous liquids. III. α relaxation,” Phys. Rev. E **72**, 011501 (2005).
- [57] Jeppe C. Dyre, “Solidity of viscous liquids. IV. Density fluctuations,” Phys. Rev. E **74**, 021502 (2006).
- [58] Jeppe C. Dyre, “Solidity of viscous liquids. V. Long-wavelength dominance of the dynamics,” Phys. Rev. E **76**, 041508 (2007).
- [59] A. J. Barlow, A. Erginsav, and J. Lamb, “Viscoelastic relaxation of supercooled liquids,” Proc. R. Soc. London **298**, 481 (1967).
- [60] A. J. Barlow, “Viscoelastic relaxation of supercooled liquids,” Adv. Mol. Relax. Proc. **3**, 256–266 (1972).
- [61] N. B. Olsen, “Scaling of β -relaxation in the equilibrium liquid state of sorbitol,” J. Non-Cryst. Solids **235**, 399–405 (1998).
- [62] J. C. Dyre and N. B. Olsen, “Minimal model for beta relaxation in viscous liquids,” Phys. Rev. Lett. **91**, 155703 (2003).
- [63] G. P. Johari, “Effect of Annealing on the Secondary Relaxations in Glasses,” J. Chem. Phys. **77**, 4619–4626 (1982).
- [64] T. Christensen and N. B. Olsen, “Determination of the frequency-dependent bulk modulus of glycerol using a piezoelectric spherical shell,” Phys. Rev. B **49**, 15396–15399 (1994).
- [65] D. Gundermann, K. Niss, T. Christensen, J. C. Dyre, and T. Hecksher, “The dynamic bulk modulus of three glass-forming liquids,” J. Chem. Phys. **140**, 244508 (2014).
- [66] U. Buchenau, “Bulk and shear relaxation in glasses and highly viscous liquids,” J. Chem. Phys. **136**, 224512 (2012).
- [67] N. L. Ellegaard, T. Christensen, P. V. Christiansen, N. B. Olsen, U. R. Pedersen, T. B. Schröder, and J. C. Dyre, “Single-Order-Parameter Description of Glass-Forming Liquids: A One-Frequency Test,” J. Chem. Phys. **126**, 074502 (2007).
- [68] N. P. Bailey, T. Christensen, B. Jakobsen, K. Niss, N. B. Olsen, U. R. Pedersen, T. B. Schröder, and J. C. Dyre, “Glass-forming liquids: One or more “order” parameters?” J. Phys. Condens. Matter **20**, 244113 (2008).
- [69] D. Gundermann, U. R. Pedersen, T. Hecksher, N. P. Bailey, B. Jakobsen, T. Christensen, N. B. Olsen, T. B. Schröder, D. Fragiadakis, R. Casalini, C. M. Roland, J. C. Dyre, and K. Niss, “Predicting the Density-Scaling Exponent of a Glass-Forming Liquid from Prigogine-Defay Ratio Measurements,” Nature Phys. **7**, 816–821 (2011).
- [70] U. R. Pedersen, N. Gnan, N. P. Bailey, T. B. Schröder, and J. C. Dyre, “Strongly Correlating Liquids and their Isomorphs,” J. Non-Cryst. Solids **357**, 320–328 (2011).
- [71] T. S. Ingebrigtsen, T. B. Schröder, and J. C. Dyre, “What is a simple liquid?” Phys. Rev. X **2**, 011011 (2012).
- [72] J. C. Dyre, “Hidden Scale Invariance in Condensed Matter,” J. Phys. Chem. B **118**, 10007–10024 (2014).
- [73] J. C. Dyre, “Simple liquids quasiuniversality and the hard-sphere paradigm,” J. Phys.: Condens. Mat. **28**, 323001 (2016).
- [74] K. Niss, D. Gundermann, T. Christensen, and J. C. Dyre, “Dynamic thermal expansivity of liquids near the glass transition,” Phys. Rev. E **85**, 041501 (2012).
- [75] U. Buchenau, “Retardation and flow at the glass transition,” Phys. Rev. E **93**, 032608 (2016).
- [76] R. Böhmer, C. Gainaru, and R. Richert, “Structure and dynamics of monohydroxy alcohols – Milestones towards their microscopic understanding, 100 years after Debye,” Phys. Rep. **545**, 125 – 195 (2014).
- [77] C. Gainaru, R. Figuli, T. Hecksher, B. Jakobsen, J. C. Dyre, M. Wilhelm, and R. Böhmer, “Shear-modulus investigations of monohydroxy alcohols: Evidence for a short-chain-polymer rheological response,” Phys. Rev. Lett. **112**, 098301 (2014).

- [78] J. C. Dyre, N. B. Olsen, and T. Christensen, “Local elastic expansion model for viscous-flow activation energies of glass-forming molecular liquids,” *Phys. Rev. B* **53**, 2171–2174 (1996).
- [79] T. Hecksher and J. C. Dyre, “A review of experiments testing the shoving model,” *J. Non-Cryst. Solids* **407**, 14–22 (2015).